



Application of an R-group search technique in the molecular design of dipeptidyl boronic acid proteasome inhibitors

JIAN-BO TONG*, YUAN-YUAN LI, GUO-YAN JIANG and KANG-NAN LI

College of Chemistry and Chemical Engineering, Shaanxi University of Science and Technology, Xi'an 710021, China

(Received 27 December 2016, revised 28 March, accepted 18 April 2017)

Abstract: In this work, a 3D-QSAR model involving for 40 dipeptidyl boronic acid proteasome inhibitors was built based on Topomer CoMFA. The multiple correlation coefficient of fitting, cross-validation and external validation were 0.908, 0.647 and 0.703, respectively. The results indicated that the obtained Topomer CoMFA model has not only the favourable estimation stability but also the good prediction capability. Topomer Search was employed as a tool for virtual screening in lead-like compounds of ZINC database. Finally, 1 R₁ group, 7 R₂ groups and 6 R₃ groups with higher contribution values were employed to alternately substitute the R₁, R₂ and R₃ of the template compound 23 with highest bioactivity. As a consequence, 33 new molecules with higher activity than that of the model molecule were designed successfully. The results showed that the Topomer Search technology could be effectively apply to screen and design new dipeptidyl boronic acid proteasome inhibitors and has good predictive capability to design new dipeptidyl boronic acid proteasome inhibitors drugs as guidance.

Keywords: quantitative structure–activity relationship (QSAR); proteasome inhibitors; Topomer CoMFA; Topomer search; design of new inhibitors.

INTRODUCTION

The prominent roles of proteasome in protein degradation has made it a promising anti-cancer drug target.^{1–3} Furthermore, some elevated levels of the proteasome have been involved in many diseases including cancer. Actually, it has been reported that the anticancer activity of proteasome inhibitors is due to the inhibition of the transcriptional factor NF-κB.^{4,5} Thus, the proteasome inhibitors are recognized as promising anticancer agents.^{6,7} The ubiquitin–proteasome pathway (UPP) plays a critical role in recognizing and degrading abnormal and misfolded proteins.^{8,9} Recent studies proved that this pathway played a critical role in the development of a series of human major diseases such as inflame-

* Corresponding author. E-mail: jianbotong@aliyun.com
<https://doi.org/10.2298/JSC161227047T>

mation, aging, cancer, neurodegenerative diseases, diabetes, etc.^{10–14} Up to now, various proteasome inhibitors have been identified and developed, and several of them are widely researched in clinical trials with possibilities for clinical applications.¹⁵ Boronic acids have been shown to be potent and specific inhibitors of serine proteases and of other enzymes.^{16,17} Boronic acid derivatives are of considerable interest in drug development because of their moderate pH of 9–10 and air-stability.¹⁸ The dipeptidyl boronic acid derivative Velcade[®], a proteasome inhibitor, was approved by the FDA in 2003 for the treatment of multiple myeloma disease.

In order to study and develop effective and novel dipeptidyl boronic acid proteasome inhibitors, novel strategies need to be considered and explored. Quantitative structure–activity relationships (QSAR) are computer-based mathematical models which combine the biological activity of compounds with theoretically calculated or experimental descriptors of their chemical structure. On the one hand, they are based on the concept that the activity of a substance is a function of its structure and can be determined on the basis of mathematical relationships developed from similar compounds, on the other hand, in comparison with other methods for assessing the toxicological effects of chemicals, such as animal-based and *in vitro* methods, QSAR models are easy to apply and efficient in terms of time and cost. In this paper, Topomer CoMFA¹⁹ model was built based on a series of dipeptidyl boronic acid proteasome inhibitors with potent inhibitor activities. A systemic external validation was applied to evaluate the correct predictive power of the model. Finally, the obtained results from topomer CoMFA, as guidance, combining with the Topomer Search²⁰ were applied to conduct ligand-based virtual screening and design new dipeptidyl boronic acid proteasome inhibitor derivatives.

MATERIALS AND METHODS

Data sets

In this paper, 40 dipeptidyl boronic acid proteasome inhibitors were taken from literature.²¹ The whole data set was randomly divided into the training set of 34 compounds for QSAR model construction and the test set of 6 compounds for model validation of the established model, and the test set as extra independent samples, were not involved in the model development.²² The IC_{50} values in the mmol range were converted to the mol (M) range and then to its logarithmic scale namely pIC_{50} ($pIC_{50} = -\log IC_{50}$) values and used as a dependent variable for further investigation. The 3D structures of 40 dipeptidyl boronic acid proteasome inhibitors were constructed using the sketch module of the SYBYL-X 2.0 package. Partial charges for all the molecules were added using the Gasteiger-Hückel method. All molecules were optimized using the tripos force field²³ and the gradient descent method with an energy charge of 0.005 kcal^{*} mol⁻¹. The maximum iteration number was 1000. The other parameters were defaulted by SYBYL-X 2.0. The structures of all the compounds along with their bioactivity values were presented in Table S-I of the Supplementary material to this paper.

*1kcal = 4186 J

Topomer CoMFA modeling

Topomer CoMFA is a second-generation comparative molecular field analysis (CoMFA)²⁴ method. The original CoMFA uses only one column, while Topomer CoMFA combine the universal “topomer” and CoMFA technologies to overcome the alignment problem of CoMFA. Topomer CoMFA is a rapid fragment-based 3D-QSAR method to predict significant R-groups of molecules, which is more efficient in forming predictive models compared with CoMFA. The Topomer CoMFA method identifies bioactivity values with the help of a compound library as a source with automated rules. Similar to CoMFA, Topomer CoMFA also needs to calculate steric and electrostatic fields at a regular space grid for substituent groups. Initially, molecule 23 was selected as the model molecule, as it had the highest activity. Finally, the fragmentation was acquired according to the compound 23. Other training molecules were identified automatically and fragmented in this style.²⁵ The molecules that were not identified needed manual fragmenting. Then the steric and electrostatic fields energy of the fragments were calculated. The chemical structure descriptors obtained were considered as the independent variables and the pIC_{50} values were regarded as the dependent variables.

In this manuscript, each structure of the training set was broken into three sets of fragments, shown as R₁ (blue), R₂ (red), and R₃ (yellow) groups and one core group to generate three-dimensional conformation. Topomer CoMFA model was built by partial least square (PLS) based on the optimum number of principal components (N)²⁶ and evaluated by leave-one-out (LOO) cross-validation.²⁷⁻²⁹ The test molecules were predicted by the Topomer CoMFA model to verify the predictive ability of the obtained model. Finally, the Compound Filed*Coeff field type was used in generating the field contour maps of the compounds.

The model was analyzed and evaluated by using some statistical parameters, including the cross-validated coefficient (q^2), the non-cross-validated correlation coefficient (r^2), standard error of estimate (SEE) and F -statistic values. It is widely accepted that the model has excellent predictive power when q^2 is more than 0.5 and the r^2 is not less than 0.6.³⁰

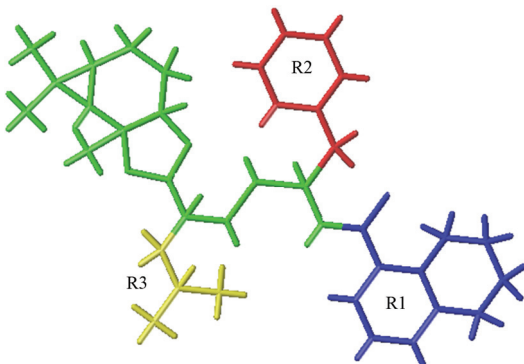


Fig. 1. Cutting style of molecule 23.

The q^2 and the r^2 of the generate model was calculated using the equations as follows:

$$q^2 = 1 - \frac{\sum(Y_{\text{pred}} - Y_{\text{obs}})^2}{\sum(Y_{\text{obs}} - Y_{\text{mean}})^2} \quad (1)$$

$$r^2 = 1 - \frac{\sum(Y_{\text{obs}} - Y_{\text{pred}})^2}{\sum(Y_{\text{obs}} - \bar{Y}_{\text{training}})^2} \quad (2)$$

where Y_{mean} means average activity value of the entire data set, while Y_{obs} , Y_{pred} and Y_{obs} represent observed, predicted and cross-validated activity values, respectively.

To validate the Topomer CoMFA derived models, the predictive ability for the test set of compounds (expressed as r^2_{pred}) was determined by using the following equation:

$$r^2_{\text{pred}} = 1 - \frac{\text{PRESS}}{SD} \quad (3)$$

where $SD = \Sigma[(\text{target data value}) - (\text{target data mean})]$; $\text{PRESS} = \Sigma[(\text{target data value}) - (\text{corresponding predicted data value})]^2$.

SD is the sum of the squared deviations between the biological activities of the test set molecules and the mean activity of the training set compounds, PRESS is the sum of the squared deviation between the observed and the predicted activities of the test set. Although not explicitly discussed, it should be noted that models have limited predictive power when the $r^2_{\text{pred}} < 0.5$.

Molecular screening

Topomer Search is a fast 3D ligand-based virtual screening tool and therefore it is able to search fragments similar to the chemical structures of the known lead compounds in large libraries of compounds. Intrinsically, it could be based on the conformational independence of Topomer similarity to carry out the whole molecule, R-groups and skeleton screening. In the present work, Topomer Search was employed to screen R-groups from ZINC molecule database (2012)³¹ with 534,597 lead-like compounds in total. Topomer distance was set as 185 to evaluate the binding degree, and other parameters were defaulted by SYBYL-X 2.0.

RESULTS AND DISCUSSION

Topomer CoMFA modeling results and evaluation

The statistic results obtained from standard Topomer CoMFA model are summarized in Table I. By observing the data of the chart, we can easily find that the r^2 value was 0.908 using 5 PLS components and the q^2 value was 0.647, F value was 55.467, r^2_{pred} value was 0.703, which indicated that the obtained Topomer CoMFA model have good predictive ability ($q^2 > 0.5$, $r^2 > 0.6$). The linear regression between the experimental pIC_{50} and the predicted pIC_{50} for the all compounds were shown in Fig. 2. The results indicated that the model does not only have favourable estimation stability, but also has good prediction capabilities.

TABLE I. The statistical results of Topomer CoMFA; N – optimal components; q^2 – the multiple correlation coefficient of cross validation; r^2 – the multiple correlation coefficient of fitting; r^2_{pred} – the multiple correlation coefficient of external validation; SEE – standard estimated error; SD – fitting standard deviation; SD_{CV} – cross-validation standard deviation

Statistical parameter	N	q^2	r^2	r^2_{pred}	SD	SD_{CV}	SEE	F
Topomer CoMFA	5	0.647	0.908	0.703	0.200	0.410	0.205	55.467

Lei and Feng *et al.* carried out 3D QSAR analysis based on CoMFA and CoMSIA (comparative molecular similarity index analysis) methods for 40

dipeptidyl boronic acid proteasome inhibitors. In this study, a fair result ($q^2 = 0.647$, $r^2 = 0.908$, $r^2_{\text{pred}} = 0.703$, $SEE = 0.205$, $F = 55.467$) was acquired with Topomer CoMFA model, which shows that the present model has favourable simulation ability, and more accurate external predictions than the former work. The Topomer CoMFA method provides an alignment independent 3D-QSAR method, which is advantageous because it is not just being alignment-independent, but it also provides the means for automated search for activity in fragment libraries. Furthermore, the introduction of Topomer CoMFA provides a brand new method to analyze substitution of a functional group rather than of a functional atom. Thus, the work performed herein has practical meaning and far-reaching influence.

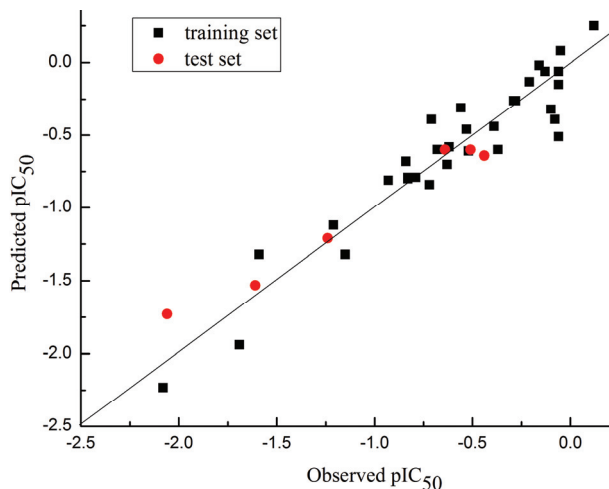


Fig. 2. Linear regression between experimental and predicted pIC_{50} values of 40 inhibitors.

3D contour plots of the Topomer CoMFA model

The three-dimensional contour plots of the Topomer CoMFA model are shown in Fig. 3a-f with the sample 23 as the reference structure. The contour maps were generated from a molecular field analysis when the Topomer CoMFA model is constructed. Contour maps can provide information about how to increase or decrease the bioactivity of the molecules, and different colours help to correlate the diversified steric and electrostatic fields with differences in the activity of the compounds. The electrostatic field contours are shown in red and blue while the steric field contours are shown in yellow and green. In the electrostatic field graph, the red and blue regions indicate the favourable electron-withdrawing groups and electron-donating groups, respectively. In the steric field graph, the green contours represent regions where a large or bulky substituent is favourable for the activity. The opposite stands for the yellow contours.

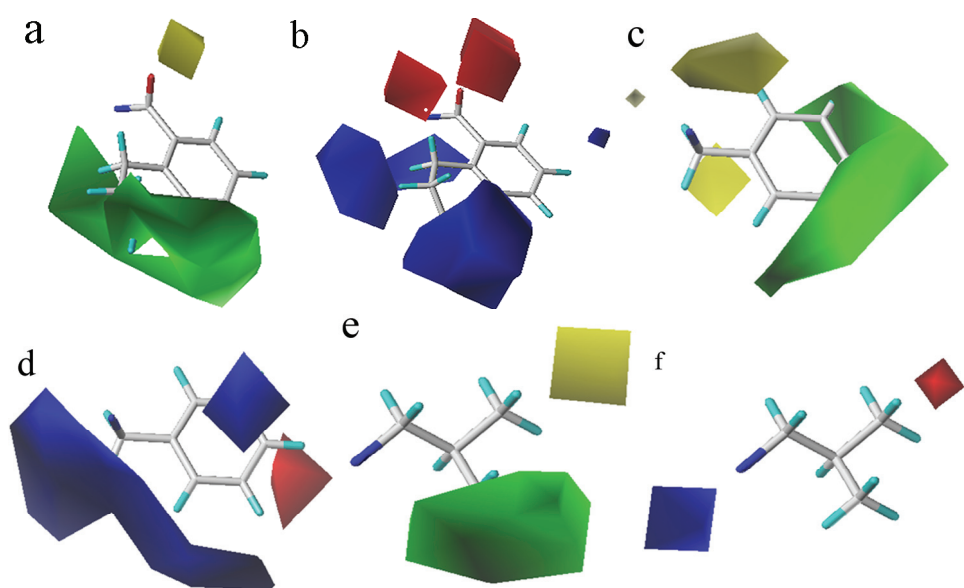


Fig. 3. 3D contour of Topomer CoMFA model: a) steric field map of R_1 ; b) electrostatic field map of R_1 ; c) steric field map of R_2 ; d) electrostatic field map of R_2 ; e) steric field map of R_3 ; f) electrostatic field map of R_3 (green and yellow contours represent steric favourable and unfavourable regions, respectively. While blue and red contours represent regions that favour electropositive and electronegative groups, respectively).

As shown in the Fig. 3a, a green contour covering the 1,2,3,4-tetrahydronaphthalene group linked to R_1 , indicates the presence of a bulky group, which is good for the biological activity. This is in agreement with the experimental data, *e.g.*, by comparing chemical structures and pIC_{50} values of compounds 1 ($pIC_{50} = -0.28$) with pyrazine group and 28 ($pIC_{50} = -0.37$) with methyl group, the compound 1 has higher activity. Moreover, the structure and activity relationship for compounds 39 ($pIC_{50} = -0.08$) and 40 ($pIC_{50} = -0.29$), compounds 20 ($pIC_{50} = -0.064$) and 29 ($pIC_{50} = -0.44$) supports this conclusion. Molecule 23 ($pIC_{50} = 0.12$) has the highest activity because of the bulky substituent at the R_1 -position. The electrostatic field contour for R_1 group (Fig. 3b) shows that the blue polyhedra region stretches around 1,2,3,4-tetrahydronaphthalene, which indicates that the electron-withdrawing group contributes to the enhancement of pIC_{50} values of molecules. However, when the chemical structures and pIC_{50} values of compounds 4 ($pIC_{50} = -0.63$) and 23 ($pIC_{50} = 0.12$) are compared, the difference in activities between compounds 4 and 23 may probably be due to some steric specificity of the receptor binding site. In Fig. 3c, there is a large blue contour around phenyl of R_2 . It can be revealed that the addition of a large volume substituent at this position increases the inhibitory activity. Comparing the compounds 21 ($pIC_{50} = -0.061$), 22 ($pIC_{50} = -0.84$) and 23 ($pIC_{50} = 0.12$), the larger

the substituent volume is, the higher is the activity of the compound, which is in accordance with the result of contour. Moreover, compounds 11 ($pIC_{50} = -1.59$), 12 ($pIC_{50} = -1.15$) and 13 ($pIC_{50} = -1.24$) also support this conclusion. Fig. 3d presents the electrostatic filed contour map of R_2 fragment. There is a large blue volume region, which indicates that a bulky electron-withdrawing group could enhance the biological activity. Compound 11 ($pIC_{50} = -1.59$) with double methyl and compound 12 ($pIC_{50} = -1.15$) with isopropyl, compound 22 ($pIC_{50} = -0.84$) with double methyl and 23 ($pIC_{50} = 0.12$) with benzene ring are also match this tendency above. In addition, the steric contour and electrostatic maps are displayed in Fig. 3e and f of R_3 fragment, respectively. The structure of R_3 group is simpler and the contribution values are smaller than the other two groups. Thus, steric and electrostatic maps are simpler than the others. According to Fig. 3e, a large green and small yellow polyhedra can be found at the side of the isopropyl, by comparing chemical structures and pIC_{50} values of compounds 5($pIC_{50} = -0.049$) and 7($pIC_{50} = -0.28$), we find the former has a large R_1 group with isopropyl, while the latter has a propyl, whose volume is smaller than that of the isopropyl, which result in a higher activity value for compound 5. This illustrates that increasing the size of the substituent at this position may increase the activity of compounds. It can be seen from Fig. 3f, a small blue contour at the side of isopropyl group, indicating that the substituent with electron-withdrawing in these regions are favourable for the improvement of molecular activity. These results are in line with the pIC_{50} values, 2 and 3 (4-methylphenyl = $-0.68 < 4$ -fluorophenyl = -0.51) where compound 2 possessed 4-methylphenyl group and displayed higher inhibitory activity than compound 3 which contained 4-fluorophenyl in R_3 -group. Compounds 9($pIC_{50} = -0.83$) and 10 ($pIC_{50} = -0.10$) support the conclusion as well.

Molecular screening and molecular design

The results of the molecular screening using the Topomer Search technology were evaluated by the Topomer distance (TOPDIST) and the contribution values of R-groups (TOPCOMFA_R). In general, R groups with higher priority contribution values were used to replace the R group of template molecular in the same limit of the TOPDIST. In this work, 1958 R_1 groups, 983 R_2 groups and 1666 R_3 groups were screened. And 92 R_1 groups and 32 R_2 groups and 333 R_3 groups with higher TOPCOMFA_R than that of template molecule were selected. Finally, the 1 R_1 group, 7 R_2 groups and 6 R_3 groups with higher contribution values were employed to alternately substitute for the R_1 , R_2 and R_3 of sample 23. Then 42 new molecules were designed. All designed 42 new molecules were optimized using the method which applied to the training molecules and their activities were predicted employing the obtained Topomer CoMFA model. The structures and activities of the 42 new compounds were

presented in Table II, from which could be seen that there are 9 new compounds with lower activities than that of the model molecule, as a result of the introduction of a smaller substituent group, or an electron-donating group into R₂ position of the template molecular. All the results are in agreement with the analysis of the 3D contour of the Topomer CoMFA model.

TABLE II. Structures and predicted pIC₅₀ values of new designed molecules

Cmpd.	Structure	Pred. pIC ₅₀	Cmpd.	Structure	Pred. pIC ₅₀
1		-0.26	22^a		0.62
2		-0.25	23^a		0.66
3		-0.26	24^a		0.65
4		-0.27	25^a		0.65

TABLE II. Continued

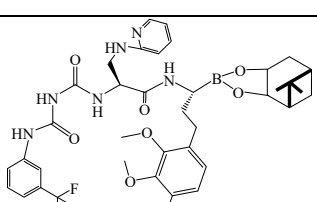
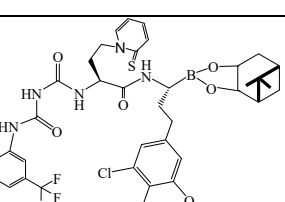
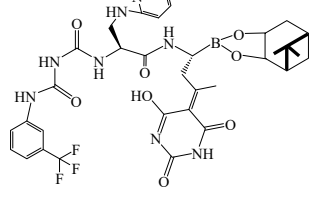
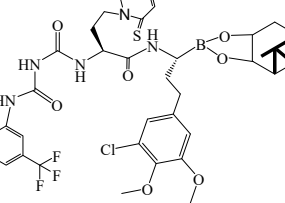
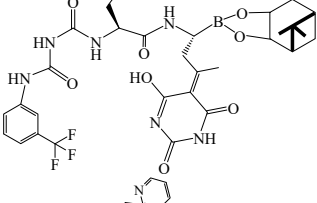
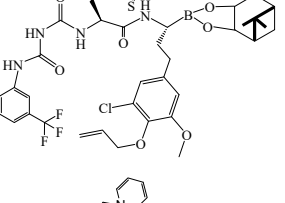
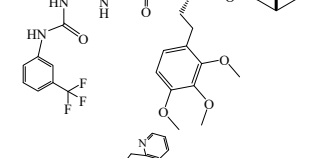
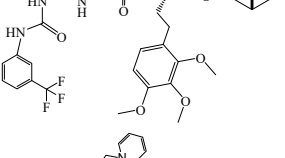
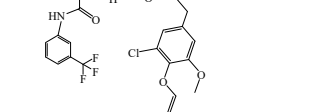
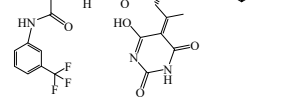
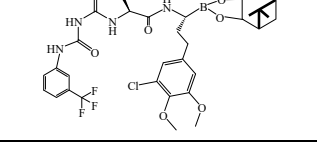
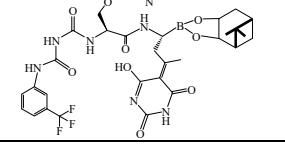
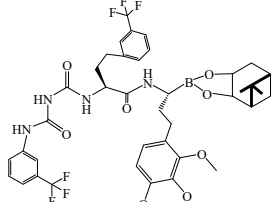
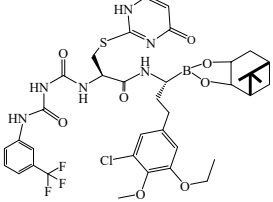
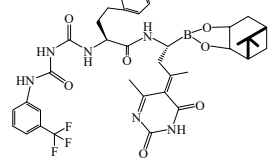
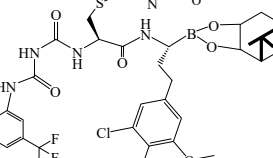
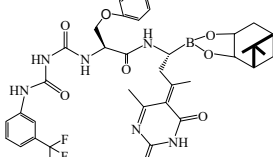
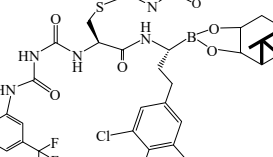
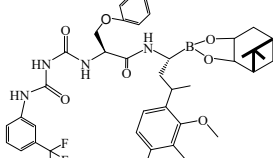
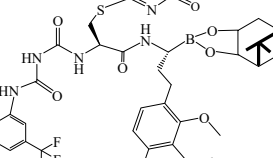
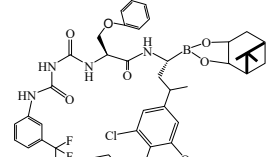
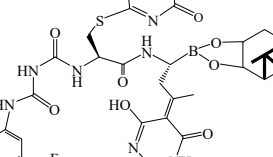
Cmpd.	Structure	Pred. <i>pIC</i> ₅₀	Cmpd.	Structure	Pred. <i>pIC</i> ₅₀
5		-0.26	26^a		0.66
6^a		0.69	27^a		0.62
7^a		0.69	28^a		0.61
8^a		0.24	29^a		0.70
9		-0.27	30^a		0.62
10		-0.26	31^a		0.62

TABLE II. Continued

Cmpd.	Structure	Pred. pIC_{50}	Cmpd.	Structure	Pred. pIC_{50}
11		-0.25	32^a		0.70
12		-0.26	33^a		0.71
13^a		0.26	34^a		0.70
14^a		0.25	35^a		0.70
15^a		0.26	36^a		0.70
16^a		0.27	37^a		0.70

TABLE II. Continued

Cmpd.	Structure	Pred. pIC_{50}	Cmpd.	Structure	Pred. pIC_{50}
17^a		0.24	38^a		0.70
18^a		0.69	39^a		0.70
19^a		0.69	40^a		0.71
20^a		0.70	41^a		0.70
21^a		0.61	42^a		0.51

^aCompounds with higher activity than that of the model molecule

CONCLUSION

In the present work, a Topomer CoMFA model with good internal and external prediction capability was established for a training set of 34 dipeptidyl

boronic acid proteasome inhibitors and a test set of 6 molecules was employed to validate the external the model predictive ability, that we have obtained. Topomer Search was used to screen R-groups in lead-like compounds of ZINC molecule database, and 33 new molecules with higher bioactivity were successfully designed based on the rule of permutations and combinations. This study provides references to drug design for the future research of dipeptidyl boronic acid proteasome inhibitors.

SUPPLEMENTARY MATERIAL

Structures and bioactivities of the 40 dipeptidyl boronic acid derivatives are available electronically at the pages of journal website: <http://www.shd.org.rs/JSCS/>, or from the corresponding author on request.

Acknowledgements. This work was supported by the National Natural Science Funds of China (21475081) (21275094), the Natural Science Foundation of Shaanxi Province of China (2015JM2057), and the Graduate Innovation Fund of Shaanxi University of Science and Technology.

ИЗВОД

ПРИМЕНА ТЕХНИКЕ ПРЕТРАГЕ R-ГРУПА ЗА МОЛЕКУЛСКИ ДИЗАЈН ДИПЕПТИДИЛБОРНЕ КИСЕЛИНЕ ИНХИБИТОРА ПРОТЕАЗОМА

JIAN-BO TONG, YUAN-YUAN LI, GUO-YAN JIANG и KANG-NAN LI

*College of Chemistry and Chemical Engineering, Shaanxi University of Science and Technology,
Xi'an 710021, China*

У овом раду је направљен 3D-QSAR модел који укључује 40 дипептидилборних киселина инхибитора протеазома на основу Торомер CoMFA. Коефицијенти вишеструке корелације, унакрсне валидације и екстерне валидације су 0,908, 0,647, односно 0,703. Резултати указују да добијени Торомер CoMFA модел не само да има повољну стабилност процењивања већ и добру способност предвиђања. Торомер Search је примењен као алат за виртуелну претрагу ZINC базе података на lead-like једињења. На крају су 1 R₁ група, 7 R₂ група и 6 R₃ група са вишим доприносима употребљене за наизменичну супституцију R₁, R₂ и R₃ шаблонског једињења 23 са највишом биоактивношћу. Као последица су успешно синтетизована 33 нова молекула са вишом активношћу од шаблонског молекула. Резултати су показали да Торомер Search технологија може да се ефикасно примени за претрагу и дизајн нових дипептидилборних киселина инхибитора протеазома и да има способност предвиђања за усмеравање при дизајну нових дипептидилборних киселина инхибитора протеазома.

(Примљено 27. децембра 2016, ревидирано 28. марта, прихваћено 18. априла 2017)

REFERENCES

1. J. Adams, *Nat. Rev. Cancer.* **4** (2004) 349
2. T. Devine, M. S. Dai, *Curr. Pharm. Des.* **19** (2013) 3248
3. R. Z. Murray, C. Norbury, *Anti-Cancer Drugs.* **11** (2000) 407
4. A. Frankel, S. Man, P. Elliott, *Clin. Cancer Res.* **6** (2000) 3719
5. J. S. Wolf, Z. Chen, G. Dong, J. B. Sunwoo, C. C. Bancroft, D. E. Capo, N. T. Yeh, N. Mukaida, C. Van Waes, *Clin. Cancer. Res.* **7** (2001) 1812

6. C. S. Mitsiades, N. Mitsiades, T. Hideshima, P. G. Richardson, K. C. Anderson, *Curr. Drug Targets.* **7** (2006) 1341
7. S. V. Rajkumar, P. G. Richardson, T. Hideshima, K. C. Anderson, *J. Clin. Oncol.* **23** (2005) 630
8. J. Shi, M. Lei, W. Wu, H. Feng, S. Chen, *Bioorg. Med. Chem. Lett.* **26** (2016) 1958
9. A. Hershko, A. Ciechanover, A. Varshavsky, *Ann. Rev. Biochem.* **67** (1998) 425
10. J. Prudhomme, E. McDaniel, N. Ponts, S. Bertani, W. Fenical, P. Jensen, K. L. Roch, *Plos One* **3** (2008) e2335
11. B. Skaug, X. Jiang, Z. J. Chen, *Ann. Rev. Biochem.* **78** (2009) 769
12. J. J. Chen, F. Lin, Z. H. Qin, *Neurosci. Bulln.* **24** (2008) 183
13. B. Dahlmann, *BMC Biochem.* **8** (2007) S3
14. J. J. Shah, R. Z. Orlowski, *Expert Rev. Anticanc.* **13** (2009) 1964
15. J. Zhang, P. Wu, Y. Hu, *Curr. Med. Chem.* **20** (2013) 2537
16. V. M. Dembitsky, A. A. Al Quntar, M. Srebnik, *Chem. Rev.* **111** (2011) 209
17. S. Touchet, F. Carreaux, B. Carboni, A. Bouillon, J. L. Boucher, *Chem. Soc. Rev.* **40** (2011) 3895
18. Y. Kong, K. Wang, M. C. Edler, E. Hamel, S. L. Mooberry, M. A. Paigea, M. L. Browna, *Bioorgan. Med. Chem.* **18** (2010) 971
19. R. D. Cramer, P. Cruz, G. Stahl, W. C. Curtiss, B. Campbell, B. B. Masek, F. Soltanshahi, *J. Chem. Inf. Model.* **48** (2008) 2180
20. R. D. Cramer, F. Soltanshahi, R. Jilek, B. Campbell, *J. Comput.-Aided Mol. Des.* **21** (2007) 341
21. M. Lei, H. Feng, C. Wang, H. Li, J. Wang, Z. Liu, S. Chen, S. Hu, Y. Zhu, *Bioorgan. Med. Chem.* **24** (2016) 2576
22. G. Melagraki, A. Afantitis, *Rsc Adv.* **4** (2014) 50713
23. M. Clark, R. D. Cramer, N. Van Opdenbosch, *J. Comput. Chem.* **10** (1989) 982
24. R. D. Cramer, D. E. Patterson, J. D. Bunce, *J. Am. Chem. Soc.* **110** (1988) 5959
25. A. Golbraikh, M. Shen, Z. Xiao, Y. D. Xiao, K. H. Lee, A. Tropsha, *J. Comput.-Aided Mol. Des.* **17** (2003) 241
26. S. Wold, *Technometrics* **20** (1978) 397
27. S. Wold, A. Ruhe, H. Wold, W. J. D. Iii, *Siam J. Sci. Stat. Comp.* **5** (1984) 735
28. L. Stähle. S. Wold, *J. Chemom.* **1** (1987) 185
29. B. L. Bush, R. B. Nachbar, *J. Comput.-Aided Mol. Des.* **7** (1993), 587
30. P. P. Roy, J. T. Leonard, K. Roy, *Chemom. Intell. Lab. Syst.* **90** (2008) 31
31. J. J. Irwin, T. Sterling, M. M. Mysinger, E. S. Bolstad, R. G. Coleman, *J. Chem. Inf. Model.* **52** (2012) 1757.